ELSEVIER

Thermochimica Acta 267 (1995) 397–404

thermochimica
acta

Heat capacity measurements of hafnium–oxygen solid solutions at high temperatures[1]

Tetsuya Kato, Toshihide Tsuji*

Department of Nuclear Engineering, Faculty of Engineering, Nagoya University, Furo-cho, Chikusa-ku, Nagoya 464-01, Japan

Received 30 November 1994; accepted 6 March 1995

Abstract

Heat capacities of hafnium–oxygen alloys, HfO_X ($X = 0.14$, 0.17 and 0.19), were measured from 325 to 905 K by using an adiabatic scanning calorimeter. A λ type heat capacity anomaly was observed around 700 K for all the samples, and was assigned to an order-disorder rearrangement of oxygen atoms. The measured values for the entropies of the order-disorder transition are in good agreement with the theoretical values in the composition range of $X \leq 1/6$ ($X = 0.14$ and 0.17), but smaller than the theoretical value in the range of $X > 1/6$ ($X = 0.19$). Another heat capacity anomaly was observed at a temperature lower than that of the order–disorder transition for the well-annealed samples. The appearance of this anomaly depends on the annealing conditions of the samples.

Keywords: Hafnium–oxygen alloy; Solid solution; Heat capacity; Order–disorder transition; Transition entropy

1. Introduction

The α phase of IVA metals namely, titanium, zirconium and hafnium, dissolves up to 29 at.% (O/Ti = 0.40) [1], 30 at.% (O/Zr = 0.43) [2] and 20 at.% (O/Hf = 0.25) [3,4] of oxygen, respectively, in the octahedral interstitial site of the hcp metal lattice. At low temperatures, the dissolved oxygen atoms form ordered structures at higher oxygen to metal ratios ($0.10 \leq X \leq 0.25$, for HfO_X) [5], and these ordered phases transform to the

---

* Corresponding author.

[1] Presented at the 30th Anniversary Conference of the Japan Society of Calorimetry and Thermal Analysis, Osaka, Japan, 31 October–2 November 1994.

SSDI 0040-6031 (95) 02497-2

disordered phases between 600 and 800 K [6,7]. The ordered structures of hafnium–oxygen solid solutions in the composition ranges of $X \leq 1/6$ and $X > 1/6$ have been determined by Hirabayashi et al. [7] by using electron and neutron diffraction methods. They have also measured the heat capacities of HfO_X ($X = 0.11–0.23$) alloys and computed the entropy of the order–disorder transition [7]. However, their experimental entropies of transition were smaller than the theoretical values calculated on the basis of their crystal structure analyses using statistical thermodynamics.

In this paper, we describe the measurements of heat capacities of HfO_X ($X = 0.14$, 0.17 and 0.19) from 325 to 905 K by using an adiabatic scanning calorimeter. The entropies of the order–disorder transition at high temperature obtained in this study are compared with the theoretical values. The transition mechanism is also discussed from the point of view of statistical thermodynamics, since the transition mechanisms for zirconium–oxygen [8] and titanium–oxygen [9] solid solutions have already been clarified by the present authors. Another heat capacity anomaly observed in the lower temperature range for the hafnium–oxygen alloys is also discussed.

2. Experimental

2.1. Sample preparation and characterization

Hafnium–oxygen alloys with O/Hf ratios of 0.14, 0.16 and 0.19 were prepared as follows. Hafnium metal sponge was oxidized for 3 h at 773 K in air and the amounts of oxygen in the oxidized hafnium were determined from the weight gain of the hafnium metal. The oxidized hafnium and hafnium metal sponge were mixed in appropriate ratios and melted a few times using a plasma jet furnace under an argon gas stream. The sample thus obtained was sealed in an evacuated silica tube, annealed for 3 days at 1273 K to homogenize the oxygen dissolved in the sample and cooled to room temperature. The homogenized ingot was crushed into pieces of less than 3 mm in size by using a stainless-steel mortar. About 36 g of the crushed sample was sealed in a quartz vessel with a helium gas pressure of 20 kPa (150 Torr) to ensure high thermal conductivity in the quartz vessel during the heat capacity measurements.

The homogenized samples were characterized using the X-ray diffraction method (XRD). All the samples prepared were single phases of hexagonal crystal structure. The lattice parameters of initial nominal compositions for all samples determined by XRD were in nearly good agreement with those reported by Hirabayashi et al. [7] and Silver et al. [10].

2.2. Heat capacity measurement

Heat capacity measurements were carried out using an adiabatic scanning calorimeter as described elsewhere [11]. In this calorimeter, the power supplied to the sample was measured continuously, and the heating rate was kept constant regardless of the nature and quantity of the sample. The heating rate chosen in this experiment was 2 K min^{-1} and the measurement was carried out from 325 to 905 K under a pressure of about 130 Pa of air in the calorimeter. Heat capacity measurements using this calorimeter were standardized by carrying out measurements on pure zirconium metal. The imprecision in the heat capacity measurements was thus determined to be +5% and the inaccuracy was determined to be ±3% in comparison with the reliable data of Douglas [12].

At first, the heat capacities of the un-annealed but homogenized samples were measured at 1273 K and heat capacity data of these samples were used for the determination of the base lines to estimate the enthalpies and entropies of transition as described later. These samples were then annealed in the temperature range of 603–623 K, for 2 weeks to form the ordered structures and cooled slowly for 1 week to ambient temperature. Finally, heat capacities of the annealed samples were again measured to determine the transition temperatures, and the enthalpies and entropies of transition for the order–disorder transition.

3. Results and discussion

The results of the heat capacity measurements on HfO_X ($X = 0.14$, 0.17 and 0.19) before and after annealing are shown in Figs. 1 and 2, respectively. In both figures, the heat capacity anomalies due to the order–disorder transitions are seen around 700 K for all the samples, although the peak areas for the samples before annealing shown in Fig. 1 are smaller than those for the samples after annealing shown in Fig. 2. We refer to it as the high temperature heat capacity anomaly in this paper. Another heat capacity anomaly is seen for the annealed $HfO_{0.14}$ and $HfO_{0.17}$ samples in the lower temperature range up to 600 K in Fig. 2. We refer to it as the low temperature heat capacity anomaly. Similar low temperature heat capacity anomalies have been observed for titanium–oxygen [9] and zirconium–oxygen [8] alloys.

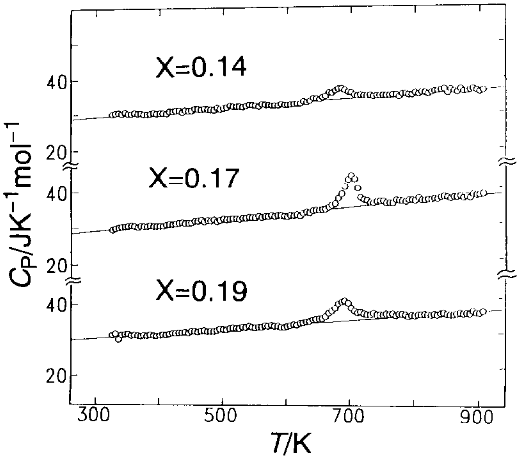

Fig. 1. Heat capacities of HfO_X ($X = 0.14$, 0.17 and 0.19) before annealing. The solid lines are the base lines determined by fitting heat capacity data without the high temperature heat capacity anomaly using a straight line.

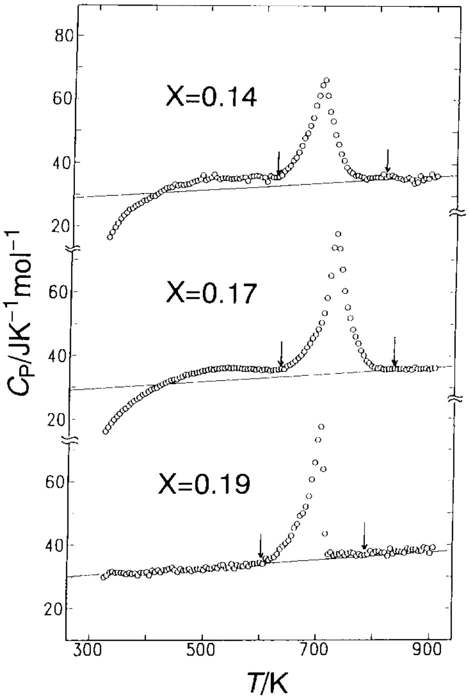

Fig. 2. Heat capacities of HfO_X ($X = 0.14$, 0.17 and 0.19) after annealing. The solid lines are the base lines of the heat capacities.

3.1. Determination of the base line of the heat capacity curve

In order to estimate the enthalpy and entropy of transition for the order disorder transition for the high temperature heat capacity anomaly, the base line of the heat capacity curve has to be determined. It is difficult to determine the base line by curve fitting heat capacity data when there is a low temperature heat capacity anomaly ($X = 0.14$ and 0.17 in Fig. 2). In these cases we use the base line of the un-annealed samples which has no low temperature heat capacity anomaly as shown in Fig. 1. The base lines of the un-annealed samples are determined by fitting the heat capacity data excluding the high temperature heat capacity anomaly to a straight line. These straight lines are shown as solid lines in Fig. 1. The slopes of these straight lines were found to be independent of the compositions of the samples within the experimental error in this work. Hence the average of these slopes was used as the slope of the base line for the annealed samples having low temperature heat capacity anomaly. The base line of each sample was determined in order to minimize the standard deviation of the heat capacity in the high temperature range above 830 K without heat capacity anomaly. In order to verify whether the method used here for the base line determination was correct, the heat capacities of un-annealed and annealed ZrO_X were measured. The base line obtained by this method agreed with the base line determined by the heat capacity analysis for zirconium–oxygen alloys [8]. For the sample of $X = 0.19$ having no a low temperature heat capacity anomaly, the straight line obtained by using a linear relationship between the temperature and heat capacity data excluding the high temperature heat capacity anomaly was used as the base line. This base line, shown as the solid lines in Fig. 2, is in good agreement with that in Fig. 1 within the experimental error.

3.2. High temperature heat capacity anomaly

The temperature corresponding to the maximum heat capacity peak in Fig. 2 is regarded as the transition temperature. The enthalpy and entropy of transition for the order–disorder transition for HfO_X are calculated on the basis of the measured heat capacity data and the base line in the temperature range shown by two arrows in Fig. 2. These arrows are determined from the shape of the peak which was found to be uninfluenced by the low temperature heat capacity anomaly. The transition temperature, enthalpy and entropy of transition obtained in this way together with those obtained previously by Hirabayashi et al. [7] are shown in Fig. 3a–c, respectively, as a function of the O/Hf ratio. The transition temperatures obtained in this study are in nearly good agreement with those measured by Hirabayashi et al. [7], but the enthalpies and entropies of transition obtained in this study are larger than those reported by Hirabayashi et al. [7]. The entropies of transition for HfO_X are theoretically calculated from configurational entropy changes for the interstitial oxygen atoms in host hafnium lattice between the ordered and disordered phases, on the basis of crystal structure. The equations [7] used for the computation are

$$\mathrm{O/Hf} \leq 1/6, \quad \Delta S = k\{\ln({}_{N-NX}\mathrm{C}_{NX})\} - k\{\ln({}_{N/6}\mathrm{C}_{NX})\}$$

$$\mathrm{O/Hf} > 1/6, \quad \Delta S = k\{\ln({}_{N-NX}\mathrm{C}_{NX})\} - k\{\ln({}_{N/6}\mathrm{C}_{N(X-1/6)})\}$$

where X, k and N are the O/Hf ratio, Boltzmann's constant and Avogadro's number, respectively. The calculated value is shown as the broken line in Fig. 3c. In Fig. 3a–c, maxima are seen near O/Hf = 1/6. The measured values for the entropies of transition in the composition region O/Hf ≤ 1/6 ($X = 0.14$ and 0.19) are in good agreement with the theoretical ones, while the experimental value in the composition region O/Hf > 1/6 ($X = 0.19$) is smaller than the theoretical one. The difference between the theoretical and the experimental data does not seem to depend on the composition region (O/Hf ≤ 1/6 or O/Hf > 1/6) of samples, since we also obtain a smaller experimental value than the theoretical one for the sample of $X = 0.14$ (O/Hf ≤ 1/6) as seen in Fig. 3c which is made at a lower annealing temperature than the appropriate temperature to form the ordered structures. It is natural that the sample annealed at lower temperature shows a lower degree of order of oxygen atoms, corresponding to a smaller transition entropy change, because a longer time is needed to obtain equilibrium state at low temperatures. Therefore, the difference between the experimental and theoretical entropy of transition may relate to a low temperature heat capacity anomaly, because all smaller entropies of tran-

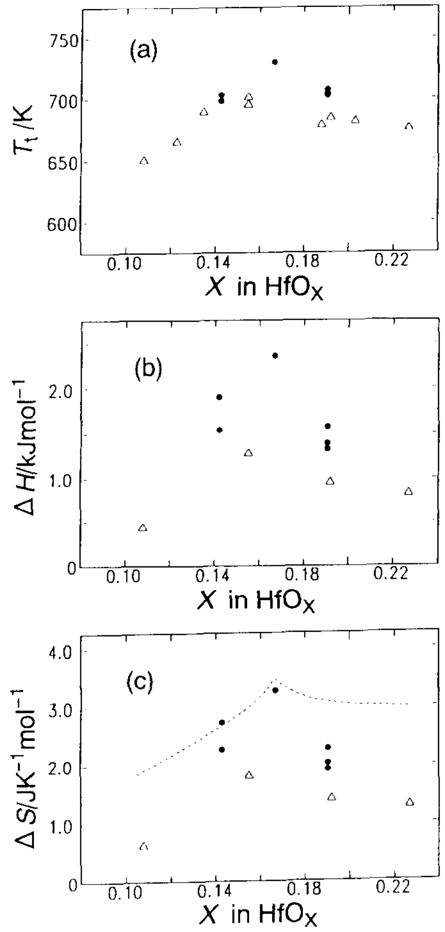

Fig. 3. (a) Transition temperatures (T_t), (b) transition enthalpy changes (ΔH) and (c) transition entropy changes (ΔS) of HfO$_X$ as a function of O/Hf ratios. ●, T_t, ΔH and ΔS in this work. △, T_t, ΔH and ΔS by Hirabayashi et al. [7]. - - - -, theoretical transition entropy change.

sition in Fig. 3c are obtained from heat capacity data without the low temperature heat capacity anomaly.

3.3. Low temperature heat capacity anomaly

The low temperature heat capacity anomaly seen in the lower temperature range up to 600 K in Fig. 2 ($X = 0.14$ and 0.17) has also been observed in our laboratory for vanadium–oxygen [13], titanium–oxygen [9] and zirconium–oxygen [8] solid solutions. In our previous paper [13], the low temperature heat capacity anomaly after annealing at high temperature had been interpreted as follows. During the cooling of the sample down to room temperature, the degree of long range order of the sample is frozen in at some temperature which is above room temperature, but is below the order–disorder transition temperature. When the temperature of such a sample with a lower degree of order than the equilibrium sample at room temperature is increased, the oxygen migration starts to induce an increase in the degree of order of the "frozen in" state at some temperature. This ordering process is exothermic and therefore the heat capacity obtained is lower than the equilibrium value. With further heating, the degree of order of the sample becomes higher than the equilibrium sample because of the time lag of interstitial oxygen migration. These processes are thought to produce an anomalous low temperature heat capacity rise at first, then the endothermic disordering process starts to produce a broad peak in the heat capacity, appearing below the main peak corresponding to the order–disorder transition temperature. This low temperature heat capacity anomaly has been observed previously in our laboratory. However, it has been found for the first time in this study that the disappearance of this low temperature heat capacity anomaly depends on the annealing conditions of the samples. It is found to be absent in un-annealed samples (as shown in Fig. 1) and in the sample annealed at a lower temperature ($X = 0.19$ in Fig. 2) as already mentioned above. Since the ordering process is expected to be observed more easily for the sample with lower degree of order (un-annealed samples in Fig. 1) than that with higher degree of order (annealed samples in Fig. 2), it may be difficult to explain only by the time lag of oxygen migration which is frozen in during cooling.

Another possible reason may be the time lag due to poor heat conduction caused by insufficient helium gas in the quartz vessel. Because the IVA metals dissolve the light elements such as oxygen [3–5], nitrogen [14], carbon [15], hydrogen [16], etc., some of the helium gas might have been absorbed in hafnium–oxygen alloys during annealing. In order to check this possibility, heat capacity was measured for the resealed sample which was sealed again with helium gas of 20 kPa in a quartz vessel without any heat treatment after confirmation of the low temperature heat capacity anomaly. This sample did not show the low temperature heat capacity anomaly. After heat capacity measurement of this sample, the helium gas was removed from a quartz vessel and the sample was sealed again in an evacuated quartz vessel. Then, the low temperature heat capacity anomaly was observed for this sample. Therefore, some of helium may be absorbed in hafnium–oxygen alloys during annealing and this may cause the time lag of heat conduction in a sealed quartz vessel, although it may be difficult apparently to consider thermal absorption of helium in hafnium–oxygen alloys during annealing.

4. Conclusions

(1) The measured values for the entropies of the order–disorder transition for hafnium–oxygen alloys, HfO_X ($X = 0.14$, 0.17 and 0.19), in the composition range of $X \leq 1/6$ ($X = 0.14$ and 0.17), are in good agreement with the theoretical values calculated by using the transition models of statistical thermodynamics on the basis of the crystal structure analyses. On the other hand, in the composition range of $X > 1/6$ ($X = 0.19$), the experimental value was smaller than the theoretical value, because the annealing tempera-

ture of the sample seemed to be lower than the appropriate temperature to obtain the ordered structure.

(2) The disappearance of the low temperature heat capacity anomaly in IVA metals was observed for the first time for hafnium–oxygen alloys in this study and the reasons were discussed.

Acknowledgements

The authors are indebted to Dr. K. Abe of Kobe Steel Ltd., Hyogo, Japan for sample preparation.

References

[1] Wehlbeck et al., J. Am. Ceram. Soc., 49 (1966) 180.
[2] J.P. Abriata, J. Garces and R. Versaci, Bull. Alloy Phase Diagrams, 7 (1986) 116.
[3] R.F. Domagala and R. Ruh, ASM Trans. Q., 58 (1965) 164.
[4] E. Rudy and P. Stecher, J. Less-Common Met., 5 (1963) 78.
[5] G. Boureau and P. Gerdanian, J. Phys. Chem. Solids, 45 (1984) 141.
[6] G.I. Ruda, V.V. Vavilova, I.I. Kornilov, L.E. Fikin and L.D. Panteleev, Inorg. Mater. USSR, 12 (1976) 396.
[7] M. Hirabayashi, S. Yamaguchi and T. Arai, J. Phys. Soc. Jpn., 35 (1973) 473.
[8] T. Tsuji, M. Amaya and K. Naito, J. Thermal Anal., 38 (1992) 1817.
[9] T. Tsuji, M. Sato and K. Naito, Thermochim. Acta, 163 (1990) 279.
[10] M.D. Silver, P.A. Farrar and K.L. Komarek, Trans. AIME, 227 (1963) 473.
[11] K. Naito, H. Inaba, M. Ishida, Y. Saito and H. Arima, J. Phys. E, 7 (1974) 464.
[12] T.B. Douglas, J. Natl. Bur. Standards. A, 67 (1963) 403.
[13] T. Matsui, T. Tsuji, T. Asano and K. Naito, Thermochim. Acta, 183 (1991) 1.
[14] E. Rudy and F. Benesovsky, Mh. Chem., 92 (1961) 415.
[15] F.A. Shunk, Constitution of Binary Alloys (2nd Suppl.), McGraw-Hill, New York, 1969.
[16] S. Yamanaka, H. Ogawa and M. Miyake, J. Less-Common Met., 172–174 (1991) 85.